Decomposition based multi-objective evolutionary algorithm for windfarm layout optimization

Article *in* Renewable Energy · August 2017

DOI: 10.1016/j.renene.2017.08.041

CITATIONS
11

READS
354

3 authors:

Partha Biswas
Nanyang Technological University
39 PUBLICATIONS **327** CITATIONS
SEE PROFILE

Ponnuthurai N. Suganthan
Nanyang Technological University
482 PUBLICATIONS **34,043** CITATIONS
SEE PROFILE

Gehan Amaratunga
University of Cambridge
749 PUBLICATIONS **26,126** CITATIONS
SEE PROFILE

Decomposition based multi-objective evolutionary algorithm for windfarm layout optimization

Partha P Biswas[1], P. N. Suganthan[1], Gehan A J. Amaratunga[2]
[1]School of Electrical and Electronic Engineering
Nanyang Technological University, Singapore
parthapr001@e.ntu.edu.sg, epnsugan@ntu.edu.sg
[2]Department of Engineering, University of Cambridge, UK
gaja1@hermes.cam.ac.uk

Abstract: An efficient windfarm layout to harness maximum power out of the wind is highly desirable from technical and commercial perspectives. A bit of flexibility on layout gives leeway to the designer of windfarm in planning facilities for erection, installation and future maintenance. This paper proposes an approach where several options of optimized usable windfarm layouts can be obtained in a single run of decomposition based multi-objective evolutionary algorithm (MOEA/D). A set of *Pareto* optimal vectors is obtained with objective as maximum output power at minimum wake loss i.e. at maximum efficiency. Maximization of both output power and windfarm efficiency are set as two objectives for optimization. The objectives thus formulated ensure that in any single *Pareto* optimal solution the number of turbines used are placed at most optimum locations in the windfarm to extract maximum power available in the wind. Case studies with actual manufacturer data for wind turbines of same as well as different hub heights and realistic wind data are performed under the scope of this research study.

Keywords: Wind turbine data · Windfarm turbine placement · Power output · Efficiency · Multi-objective evolutionary algorithm · Hub heights.

1. Introduction

Enormous growth in renewable energy is anticipated in electric sector for a sustainable future and for stricter norms imposed on carbon emission. A popular, fast growing form of naturally replenished renewable energy is the wind energy where the power in the wind is extracted by the turbine through rotation of its blades. Wind turbines, in general, are installed in a cluster at a potentially windy site. However, careful study and judgement are pre-requisites to place the wind turbines in a windfarm as wake loss induced by upstream turbines affect the output of downstream turbines, thereby reducing total power output from the windfarm. Mosetti *et al.* [1] proposed binary coded genetic algorithm (GA) to optimize windfarm layout with objective of minimizing cost per unit power output (e.g. cost per kW) from the windfarm. Grady *et al.* [2] improved the results employing same method but with higher number of generations. Mittal [3] in his research showed fine grid spacing in windfarm could further increase the power output. Emami *et al.* [4] took weighted sum approach of the objective function consisting of both cost and power. Marmidis *et al.* [5] adopted Monte Carlo simulation method to study single objective of cost per unit power output for simplest wind condition. Binary particle swarm optimization with time varying acceleration coefficient (BPSO-TVAC) in ref. [6] showed competitive results on windfarm layout optimization with objective of cost per kW. Literature [7] performed the same layout optimization using linear population size reduction technique of success history based adaptive differential evolution (L-SHADE) algorithm and claimed to have obtained best results among comparable studies on single objective optimization. Ant colony optimization (ACO) algorithm, a co-operative agent approach was proposed in [8]. Greedy algorithm with consideration of levelized cost of energy (LCOE) was studied in [9]. Literature [10] performed windfarm layout optimization using same greedy algorithm for multiple hub heights of wind turbines. Global windfarm cost model incorporating initial investment and yearly income on net generated energy was established in [11]. Analytical modelling of windfarm with multi-level extended pattern search was presented in [12]. All these literatures considered optimization of single objective of either maximizing power output or minimizing cost per kW. Furthermore, literatures [1-8] adopted simplified cost model proposed in [1] where cost was considered to be a function of only number of turbines in the windfarm. Ref. [13] performed case studies to maximize windfarm efficiency with different rotor diameters and hub heights. In summary, literatures on windfarm layout optimization mostly consider varying single objective, sometimes alongwith simplified cost model.

Multi-objective genetic algorithm (MOGA) based optimization of windfarm is proposed by Chen *et al.* [14]. However, the authors in [14] have focused only on a specific value of installed capacity. In other words, mainly one *Pareto* solution is utilized in the optimization process. The validity and usefulness of complete *Pareto front* (i.e. all

non-dominated solutions in the multi-objective optimization) are not discussed. Ref. [15] adopted multi-objective random search algorithm with optimization objectives being number of turbines and cable length. The *Pareto front* in [15] is found to be quite narrow and irregular with all solutions being not feasible as mentioned in the paper. Our research presented in this paper approaches the windfarm layout optimization problem using multi-objective evolutionary algorithm based on decomposition (MOEA/D) [16,17]. MOEA/D uses the method of decomposing a multi-objective optimization problem into several scalar optimization subproblems and optimizes those simultaneously. Reference [16] justified and proved the advantages of this algorithm over other comparable algorithms. As each subproblem is optimized by only using information from its neighboring subproblems, the computational complexity of MOEA/D is less than multi-objective genetic local search (MOGLS) and nondominated sorting genetic algorithm-II (NSGA-II). Disparate objectives can simply be normalized when applying the algorithm MOEA/D. For the problem of windfarm layout optimization, maximizing both power output and windfarm efficiency are considered as two objectives in MOEA/D algorithm. The objectives framed in this way help to obtain several *Pareto* optimal solutions in a single run of the algorithm. As all solutions are theoretically usable, the designer can make an appropriate selection from a pool of closely matched optimized solutions considering factors like installed capacity, budget and site constraints. Our selection and proposal of *Pareto* optimal layouts are for installed capacity based on statistical data of commercial wind turbine sites presented in [18]. Vestas V80-2.0MW model turbine data are used to optimally place in a rectangular shaped windfarm with specified number of cells. Detailed case studies with same and different available hub heights for the wind turbines are performed. The wind condition in this study considers a couple of realistic cases of variable wind speed and direction in line with the windroses for the month of April in Midland and Corpus Christi, Texas [19].

In organizing rest of the paper, the authors introduce the mathematical models and numerical data used for the windfarm in section 2, approach and application of the algorithm in placement optimization in section 3, description and results of the case studies in section 4, followed by conclusion and close out remarks in section 5.

2. Mathematical models and numerical data

2.1. Linear wake model

As wind flows across a turbine, the wind speed decreases and turbulence intensity increases; thus forming a wake behind the turbine. The wake not only continues to move in the downstream direction, it also expands laterally. Because of wake effect, turbines located downstream generate less power. Out of several wake models, popular and extensively used Jensen wake decay model [20,21] is adopted here for consideration of wind velocity inside the wake region. In the equations below for clarity k-th turbine is considered under the influence of single turbine at m-th location (Fig. 1a). Assuming that the momentum is conserved in the wake, the wind speed in the wake region is calculated by [13] –

$$u_k = u_{0k}\left[1 - \frac{2a}{\left(1 + \alpha_m \frac{x_{mk}}{r_{m1}}\right)}\right] \tag{1}$$

$$a = \frac{1 - \sqrt{1 - C_T}}{2} \tag{2}$$

$$r_{m1} = r_m \sqrt{\frac{1 - a}{1 - 2a}} \tag{3}$$

$$\alpha_m = \frac{0.5}{\ln(\frac{h_m}{z_0})} \tag{4}$$

where, u_{0k} is the local wind speed at k-th turbine without considering the wake effect; x_{mk} is the distance between m-th & k-th turbine; r_m is the radius of m-th turbine rotor; r_{m1} is the downstream rotor radius of m-th turbine; h_m is the hub height of the m-th turbine; α_m is the entrainment constant pertaining to m-th turbine; a is the axial induction factor; C_T is the thrust coefficient of the wind turbine rotor; z_0 is the surface roughness of the windfarm.

The wake region is conical for linear wake model and radius of the wake region is represented by wake influence radius defined as:

$$r_{wm} = \alpha_m x_{mk} + r_{m1} \tag{5}$$

Local wind speed at k-th turbine is dependent upon the hub height of the turbine as velocity of wind changes with height from ground. Logarithmic law has been used here to represent the local wind speed.

$$u_{0k} = u_{ref} \log\left(\frac{h_k}{z_0}\right) / \log\left(\frac{h_{ref}}{z_0}\right) \tag{6}$$

where, h_{ref} is the reference height and u_{ref} is the wind speed at reference height

When one area is inside multiple wake flows, the velocity deficit will be enhanced. If we consider i-th turbine under the influence of multiple wakes, taking into account the wake flow superimposed effect, the wind speed at the position of i-th turbine can be written as:

$$u_i = u_{0i}\left[1 - \sqrt{\sum_{j=1}^{N_t} \frac{A_{ij}}{\pi r_i^2}\left(1 - \frac{u_{ij}}{u_{0j}}\right)^2}\right] \tag{7}$$

where, u_{0i} & u_{0j} are the local wind speeds (free stream velocity) at i-th & j-th turbines, respectively without considering the wake effect; u_{ij} is the wind velocity at i-th turbine under the influence of j-th turbine; N_t is the number of turbines affecting the i-th turbine with wake effects; r_i is the rotor radius of i-th turbine; A_{ij} is the overlapped rotor area of i-th turbine under wake influence radius (r_{wj}) of j-th turbine (Fig. 1b). Under full wake condition, $A_{ij} = \pi r_i^2$.

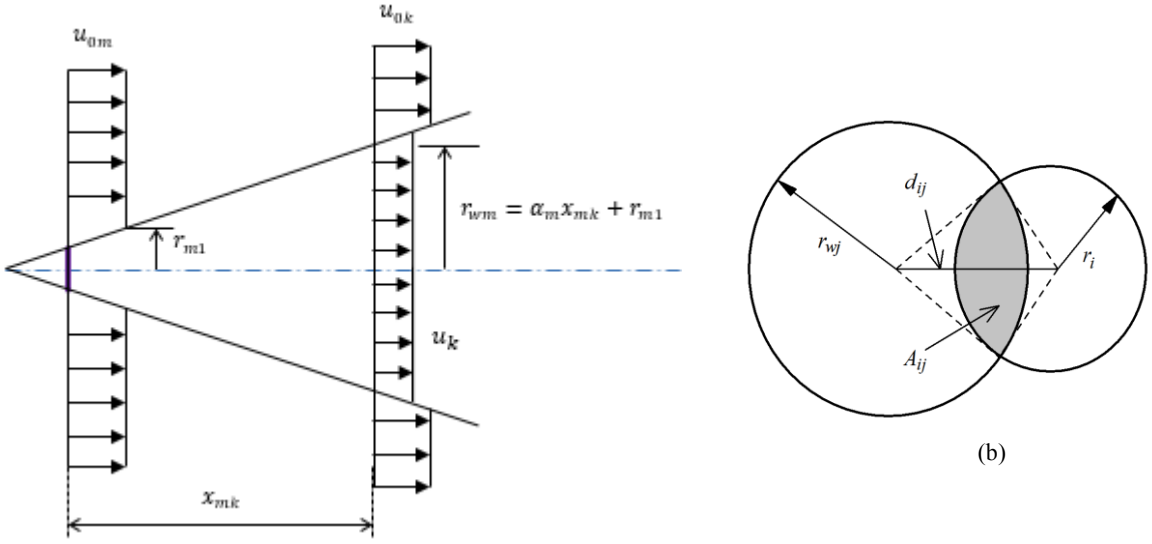

Fig. 1: (a) Linear Wake Model - k-th turbine under the influence of single m-th turbine (b) i-th turbine partially influenced by wake radius r_{wj} of j-th turbine

2.2. Turbine power output model

Power output curve of Vestas V-80 model, which has a rotor diameter of 80m, is used here to calculate output power from the turbine. The curve is reproduced in Fig. 2 with fairly accurate liner approximation. Mathematically the power model in kW as a function of wind speed, *u* can be expressed as:

$$P(u) = \begin{cases} 0, & \text{for } u < u_c \\ 60 * (u - u_c), & \text{for } u_c \le u < u_c + \frac{25}{19} \\ 250 * (u - u_c - 1), & \text{for } u_c + \frac{25}{19} \le u \le 13 \\ 2000, & \text{for } 13 < u \le u_f \\ 0, & \text{for } u > u_f \end{cases} \tag{8}$$

where, u_c and u_f are the cut-in and cut-out wind speeds of the turbine, respectively.

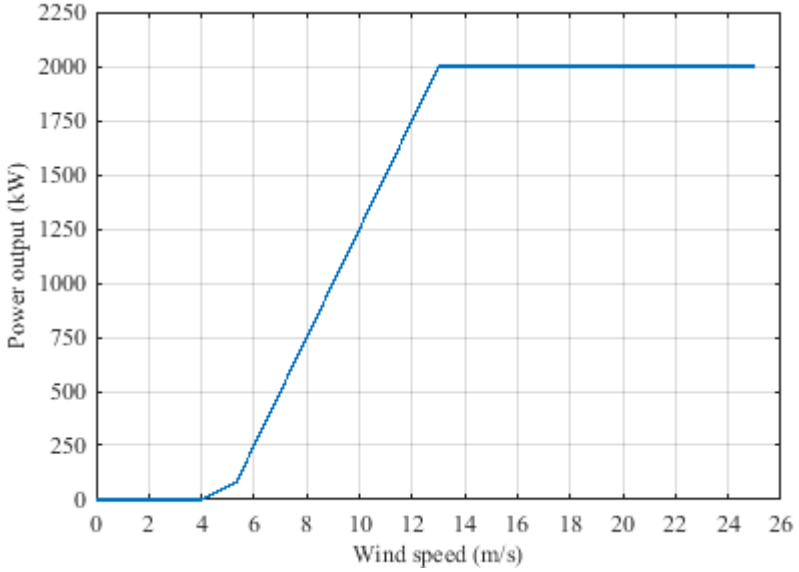

Fig. 2: Linear approximation of power output curve for Vestas V-80 turbine

2.3. Wind condition model

Constant speed and fixed direction of wind condition is good for theoretical study purpose. However, this situation hardly exists in real world. Many previous research papers considered a constant wind speed of 12m/s at hub height from either single or multiple directions. Standard [22] stipulates the design requirement of wind turbines and defines highest turbulent class IA of the turbine which is certified to perform for maximum annual average wind speed of 10m/s at hub height. So, a constant wind speed of 12m/s at hub height is a hypothetical case for which technical feasibility, economic viability and practical applicability seem yet to be determined. In this paper, the authors suggest a couple of wind probability distribution diagrams in line with the windroses for the month of April of sites in Midland and Corpus Christi, Texas [19]. We designate Midland as site 1 and Corpus Christi as site 2. The selected locations are considered to be high potential sites for wind energy. Instead of discretizing the wind speeds in 1 m/s, an approximation with four dominant discrete wind speeds is made in the wind probability distribution diagrams in Fig. 3 and Fig. 4 for site 1 and site 2 respectively. North (N) direction is set as 0° and an increment of 22.5° in clockwise direction is considered to divide 360° in 16 segments. In each of these 16 directions, the probability of occurrence of each discrete wind speed is indicated in the bar chart. The summation of all the probabilities equals 1. As observed from the wind distribution diagrams, for site 1 in Midland, the wind is dominant from south direction while for site 2 in Corpus Christi, high intensity wind blows from south-east direction with negligible wind from west direction.

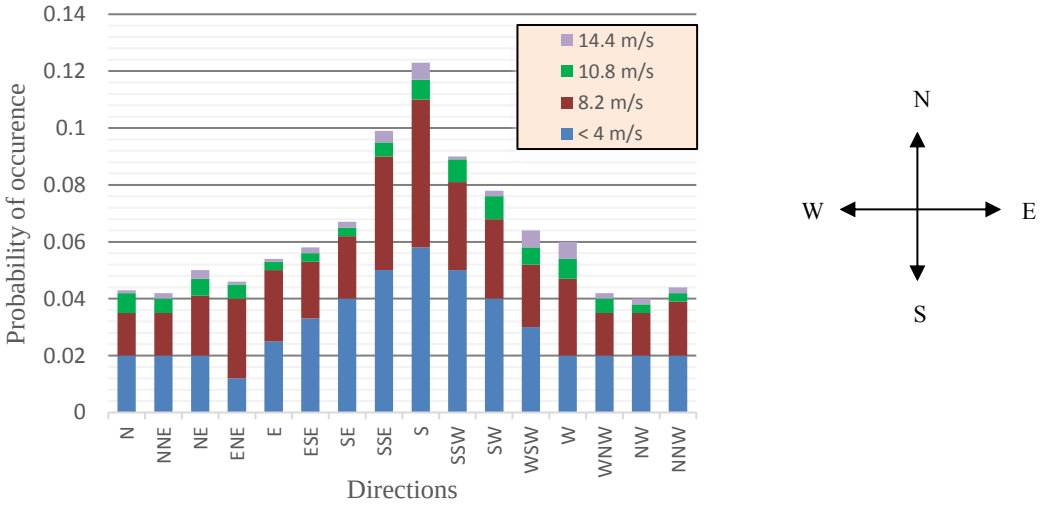

Fig. 3: Wind probability distribution diagram 1 for site 1 – Midland, Texas

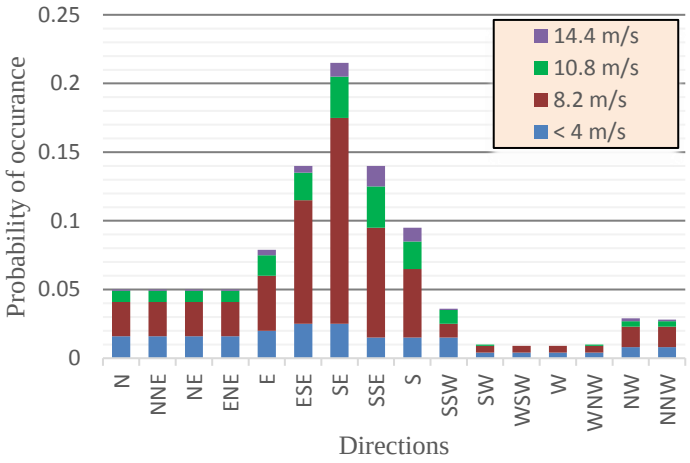

Fig. 4: Wind probability distribution diagram 2 for site 2 – Corpus Christi, Texas

2.4. *Objective model*

Efficiency of the windfarm is calculated by,

$$\eta = \frac{\sum_{k=0}^{360}\sum_{i=1}^{N_T} f_k P_i(u_i)}{\sum_{k=0}^{360}\sum_{i=1}^{N_T} f_k P_{i,max}(\overline{u_i})} \tag{9}$$

where, N_T is the total number of turbines, $P_{i,max}$ is the maximum power output from i-th turbine as a function of wind speed $\overline{u_i}$ had there been no wake effect, P_i is the actual power output from i-th turbine as a function of wind speed u_i considering wake effect it experiences from upstream turbine(s). The probability of occurrence of each wind speed from each direction is defined by factor f_k and $\sum_{k=0}^{360} f_k = 1$.

Total power output of the windfarm is given by,

$$P_{total} = \sum_{k=0}^{360}\sum_{i=1}^{N_T} f_k P_i(u_i) \tag{10}$$

Instead of single objective function used in most of previous studies, multi-objective using MOEA/D algorithm is proposed in this paper. Two objective functions are defined as, (a) maximize power output $'P_{total}'$ and (b) maximize efficiency $'\eta'$. A careful observation on the objectives reveal that increasing number of turbines will increase power output from the windfarm. However, as more and more turbines are added to the designated cells, wake effect starts to increase bringing the overall efficiency of the windfarm down. Fewer turbines in the windfarm will result in minimum or almost zero wake loss. So, effectively designer has to choose an acceptable value of overall efficiency on desired installed capacity. When placement optimization is performed for a defined area, MOEA/D provides *Pareto* optimal set containing all possible layouts ranging from layouts that provide maximum possible power output at lowest (but maximum achievable) efficiency to layouts that provide minimum power output at highest efficiency of very close to 100%. To elaborate further, any *Pareto* optimal point will contain information on number of turbines with best possible layout arrangement that minimizes wake loss.

Several research papers have considered cost or cost per unit power output as the objective. Though the cost model as a function of only number of turbines, proposed by Mosetti *et al.* [1], is widely used in literature, the basis of such model is not proven with actual data. Chen *et al.* [14] applied JEDI model which has turbine rated power, number and type of turbines in a windfarm as variables. The JEDI model can be interpreted as a model developed based on statistical analysis of wide range of data including cost of land lease, job market, labor cost etc. Chen *et al.* [23] proposed another cost model which considers cost of wind turbine hub as a percentage of total cost of the turbine. However, this cost model [23] considers only installed cost of turbines. Cost of wind power is evaluated based on levelized cost of energy (LCOE) [24]. LCOE is calculated over a period of time of the wind farm accounting initial installation, erection and commissioning cost, annual fixed charge rate (FCR), annual operation and maintenance cost etc. and the energy produced by the farm. Due to limited availability of publicized commercial price of turbines, it is difficult to quantify cost of wind turbine hub only as a small difference in hub height may have insignificant impact on LCOE. Nevertheless, intuitively it can be assumed that turbines with higher hub heights will cost more than those with lower hub heights. Our algorithm picks shorter hub heights for the turbines with equal probability for evaluation, although any simplified cost model is not set as a primary objective for optimization.

2.5. *Windfarm selection and turbine data*

A rectangular windfarm of 6000m x 2000m is considered for all case studies performed under the scope of this literature with each cell size being 300m x 400m. The grid size is thus selected because commercial turbines are hardly placed near to each other [18,25] and Jensen wake decay model [20,21] is applicable for far wake region in the downstream of a turbine, a distance beyond two to five times the rotor diameter of the turbine depending on ambient turbulence [25]. A turbine can be placed at the center of any cell, which means there are maximum 100 possible locations where the turbine can be positioned. Grid spacing thus selected will also ensure minimum safe distance between any two turbines. The safe distance is defined as the minimum distance if followed while placing the turbines in a windfarm, will ensure that falling accidentally down of one turbine does not cause damage to the others [10]. The turbine and other relevant data used for calculation are listed in Table 1. Vestas V-80 wind turbine is one of the popular turbine models and selected herein for study purpose. Power output characteristic curve and various turbine speeds (i.e. cut-in, cut-out and rated speeds) do not vary much for different make of 2-MW turbine model. As an obvious fact, the output power of a windfarm changes with the change in turbine type, size and wind characteristic of the site. In general, larger turbine rotor diameter and higher hub height would produce more power output if available in the wind.

Table 1:
Turbine and other relevant data.

Parameter	Value
Turbine model	Vestas V-80
Rated power, P_{rated}	2000 kW
Rotor diameter, D	80 m
Thrust coefficient, C_T	0.8
Hub height (IEC IA) [22]	60 m, 67 m or 78 m
Cut-in speed, u_c	4 m/s
Cut-out speed, u_f	25 m/s
Surface roughness of windfarm, z_0	0.3 m
Reference height, h_{ref}	60 m

3. Application of decomposition based multi-objective evolutionary algorithm

3.1. *Introduction and formulation of decision vector*

Multi-objective evolutionary algorithm (MOEA/D) decomposes a multi-objective optimization problem (MOP) into a number of scalar optimization subproblems and optimizes them simultaneously [16]. The multi-objective optimization (MOP) for the problem applied here is defined as:

Minimize $F(x) = \{f_1(x), f_2(x)\}$ where, $f_1(x) = -'P_{total}'$ and $f_2(x) = -'\eta'$

Variable $x \in \Omega$, Ω being the decision vector (variable) space. If N is the population size, there will be N decision vectors $x^1, x^2, \ldots, x^N$ for the optimization problem. The windfarm has 100 possible locations where the turbines can be placed. Each decision vector x^m for $m = 1,2, \ldots, N$ is formulated as a 100-dimensional vector with each of the element assuming a discrete integer value representing status of that location. For only one type of turbine in the windfarm, each element of m-th vector x^m adopts a discrete value of either 0 or 1 i.e. $x_k^m \in \{0,1\}$ for $k = 1,2, \ldots, 100$. '0' means the location is empty while '1' indicates the location has a turbine. For the case where 3 different variants of hub heights are present, $x_k^m \in \{0,1,2,3\}$ for $k = 1,2, \ldots, 100$. Again, '0' means the location is empty while '1, 2 or 3' indicates the variant for the turbine at that location. For both the cases, random initialization of x is done with probability of selection of '0' set at 75%, while other integer value(s) is(are) equally likely to be initialized with remaining probability. This helps to obtain low power output solutions when the number of turbines are very few in the windfarm and possibly drop some impracticable solutions when the windfarm occupancy is close to 100%. During evolution through mutation and crossover the value of any x element may become a fraction in which case it is rounded off to the nearest integer value.

3.2. *Pareto optimality*

If R^2 is the objective space for 2 objectives, for $x \in \Omega$, $F(x) \in R^2$. Now, say u, v are two objective vectors in the objective space. u is said to dominate v if and only if $u_i \leq v_i$ for every $i \in \{1,2\}$ and $u_j < v_j$ for at least one index $j \in \{1,2\}$. A point $x^* \in \Omega$ is a *Pareto optimal* if there is no point $x \in \Omega$ such that $F(x)$ dominates $F(x^*)$ [17]. $F(x^*)$ is termed as the *Pareto optimal (objective) vector*. To elaborate further, any effort in improving *Pareto optimal* point in one objective must lead to worsening of the other objective in a two-objective optimization

problem. *Pareto set* (PS) is the set of all the *Pareto* optimal points and *Pareto front* (PF) is the set of all the *Pareto* optimal objective vectors [26].

3.3. *Decomposition approach*

MOEA/D decomposes the approximation of PF into several scalar optimization subproblems [27]. Among few variants of MOEA/D, the one with dynamic resource allocation (MOEA/D-DRA) [17] is adopted here. N evenly spread weight vectors, $\lambda^1, \lambda^2 \ldots . \lambda^N$ are required to decompose the MOP. In this specific problem of windfarm layout optimization, $N = 600$ is considered with each weight vector being of 2 dimensions for the two objectives i.e. $\lambda^m = (\lambda_1^m, \lambda_2^m)^T$ for $m = 1,2,..,N$ and $\lambda_1^m + \lambda_2^m = 1$.

Suppose $z^* = (z_1^*, z_2^*)^T$ is the minimum objective value vector that will be treated as reference point and the elements of this vector are calculated as $z_1^* = \min\{f_1(x)|x \in \Omega\}$ and $z_2^* = \min\{f_2(x)|x \in \Omega\}$. After decomposition of MOP into N subproblems, the objective function of m-th subproblem is:

$$g^{te}(x|\lambda^m, z^*) = \max\begin{Bmatrix}\lambda_1^m|f_1(x) - z_1^*|\\ \lambda_2^m|f_2(x) - z_2^*|\end{Bmatrix} \tag{11}$$

z^* is all likely to be unknown beforehand. During the search process, the algorithm uses the lowest values of $f_1(x)$ and $f_2(x)$ found thus far to substitute z_1^* and z_2^*, respectively in the objectives of the subproblems. MOEA/D performs simultaneous minimization of all N objective functions (for N subproblems) in a single run. Each subproblem is optimized by utilizing information mainly from its neighboring subproblems. In MOEA/D, all subproblems are given equal computational effort. However, MOEA/D-DRA algorithm is designed to give varying computational efforts on different subproblems based on utility values of the subproblems [17].

The objectives in windfarm problem are highly disparate as power output $'P_{total}'$ can take values of tens of MW, while efficiency values lie between 0 and 1. Normalization of the objectives is necessary in MOEA/D, else the algorithm may evolve towards the objective with higher numerical value. The normalization process brings the values of both objectives within the range 0 to 1. It is implemented by modifying the decomposed objective function in equation (11) as:

$$g^{te}(x|\lambda^m, z^*, z^{nad}) = \max\begin{Bmatrix}\lambda_1^m\left|\frac{f_1(x) - z_1^*}{z_1^{nad} - z_1^*}\right|\\ \lambda_2^m\left|\frac{f_2(x) - z_2^*}{z_2^{nad} - z_2^*}\right|\end{Bmatrix} \tag{12}$$

where, $z^{nad} = (z_1^{nad}, z_2^{nad})^T$ is the vector of maximum values of $f_1(x)$ and $f_2(x)$ and similar to z^*, z^{nad} is also evaluated by the algorithm during the search process using maximum values of $f_1(x)$ and $f_2(x)$ [29].

During the search process MOEA/D-DRA with Tchebycheff approach [26] maintains:

- A population of N vectors $x^1, x^2, \ldots, x^N$ and in this specific problem each vector contains 100 elements.
- Function values of $FV^1, FV^2, \ldots, FV^N$ where $FV^m = \{f_1(x^m), f_2(x^m)\}$ for $m = 1,2, \ldots, N$.
- $z^* = (z_1^*, z_2^*)^T$, where z_1^* and z_2^* are the minimum values found thus far evaluating $f_1(x)$ and $f_2(x)$.
- $z^{nad} = (z_1^{nad}, z_2^{nad})^T$, where z_1^{nad} and z_2^{nad} are the maximum values found till now evaluating functions $f_1(x)$ and $f_2(x)$.
- Utility of the subproblems, π^m for $m = 1,2, \ldots, N$.
- Current generation number *gen*.

3.4. *MOEA/D-DRA algorithm*

Input: (i) MOP (ii) a stopping criterion, *Maxeval* (iii) Number of subproblems, N (iv) A uniform spread of N weight vectors, $\lambda^1, \lambda^2 \ldots ., \lambda^N$ (v) T: the number of the weight vectors in the neighborhood of each weight vector.

Output: $\{x^1, x^2, \ldots ., x^N\}$ and $\{f_1(x^m), f_2(x^m)\}$ for $m = 1,2, \ldots ., N$.

Step 1 - Initialization: Initialize decision vectors as described in section 3.1. Initialize N uniformly spread weight vectors, z^*, z^{nad}. Compute Euclidean distance between any pair of weight vectors to define T-neighbors of each weight vector. Set generation counter *gen = 0* and utility function $\pi^m = 1$ for all subproblems.
Step 2 – Selection of subproblems and update of solutions: For each weight vector, its N_S neighborhood is the set of N_S closest weight vectors (by Euclidean distance) to it. Now, each subproblem is associated with a solution and a weight vector. Two subproblems are said to be neighbors if their weight vectors are also neighbors. In a generation, selection of subproblems is done based on utility values using 10-tournament selection method [17] and

20% subproblems are identified in the process in each generation. A set of the current solutions corresponding to the selected indices of subproblems is picked up in that generation. For each selected solution x^m, MOEA/D-DRA performs following tasks [27]:

1. Set the mating and update range P to be the T-neighborhood of x^m with a large probability δ, and the whole population otherwise.
2. Randomly select three current solutions from P.
3. Apply genetic operators with pre-defined crossover rate CR and mutation factor F on the above selected solutions to generate a new solution y [17]. Check range bounds for y and repair if necessary. Compute objective $F(y)$.
4. Replace a small number (n_r) of solutions in P by y if y yields better than current FV of related subproblem.

No solution will be replaced in step 4 if y is not better than any solution in P for its subproblem. The update is said to be a failure when such a case happens, else, it is successful.

Step 3 – Stop if stopping criterion i.e. *Maxeval* is reached.
Step 4 – *gen* = *gen+1*. Update the utilities of subproblems when *gen* is a multiplication of 50 [17]. Go to **Step 2**.

The algorithm is developed on MATLAB software platform and simulations are run on a computer with Intel Core i5 CPU @2.7GHz and 4GB RAM. The selected parameters of MOEA/D for current problem are given in Table 2.

Table 2:
MOEA/D optimization data

Parameter	Value
Population size, *N*	600
Number of weight vectors, *N*	600
Neighborhood size, *T*	0.1*N*
Probability to update the neighbor (else the whole population), δ	0.9
Max number of positions replaced by better new solution in each subproblem at every generation, n_r	0.01*N
Maximum number of function evaluation, *Maxeval*	300000
Crossover rate, *CR*	0.5
Mutation factor, *F*	0.5
Distribution index [17]	20

4. Case studies

A total of four case studies for two different wind conditions together with detail analysis of results are included in this section for the rectangular windfarm. The first two case studies consider same hub heights for all the turbines while in the remaining cases we let the algorithm choose best suited hub heights to maximize power and efficiency. Turbine cost is not set as a primary objective of optimization. Hence, in latter cases, it is anticipated that the algorithm will have a tendency to choose higher hub heights for the turbines as wind speed at higher altitude is more than that at lower altitude. However, power output saturates at rated power of the turbine, so it cannot be forthrightly concluded that increasing tower height is always beneficial to extract more power. Probability and direction of different wind speeds, setting of the turbines are the factors affecting power output from a windfarm. Painstaking effort and time is required even for an algorithm to do the number crunching and successfully find an optimal solution. MOEA/D algorithm effectively performs the task of optimization and in a single run it proposes a set of closely optimized solutions so that the designer can make a choice best suited to his planning.

4.1. Case 1 and case 2 (same hub height)

Study cases 1 and 2 consider same tower (hub) height of 60m for all turbines for wind conditions at site 1 and site 2 respectively. Four discrete wind speeds as per wind distribution diagram in Fig. 3 and Fig. 4 are considered at reference height of 60m. In summary, $u_{ref0} < 4$m/s, $u_{ref1} = 8.2$m/s, $u_{ref2} = 10.8$m/s and $u_{ref3} = 14.4$m/s at $h_{ref} = 60$m. A cursory glance at turbine power curve reveals that the turbine delivers its peak rated power at a wind speed of 13m/s. Wind speed beyond that does not increase power output and the turbine delivers same rated output till cut-out wind speed is reached. Wind velocity encountered by a wind turbine under influence of wake is determined by equations (1) to (7). Power output and objective functions are calculated using equations (8) to (10). After setting the parameters of MOEA/D, the optimization algorithm is run for 10 times for each study case to check consistency of results. The plots of *Pareto fronts* i.e. non-dominated solutions for objectives (total 600 points) of the selected runs are shown in Fig. 5 and Fig. 6 for wind characteristics at site 1 and site 2 respectively. Windfarm being a discrete location optimization problem, all non-dominated solutions may not be unique and wind probabilities being random, the *Pareto front* curves may not always be smooth. Addition or removal of any turbine will change power output and efficiency to an extent depending upon the location to where it is added or from where

it is removed. Nonetheless, the curve presents an obvious fact of decrease in efficiency with increase in output power (i.e. increase in number of turbines). Number of turbines for each solution versus the corresponding power output at achievable efficiency is plotted in Fig. 7 for case 1 and Fig. 8 for case 2. In general, slightly higher efficiency is observed with same number of turbines for wind condition at site 2. This is because greater probabilities of higher wind speeds at site 2 help to generate more power output from the turbines. The algorithm provides optimal layouts for each discrete number of turbines over a wide range. For example, in case 1, the *Pareto* front corresponds to optimal layouts with number of turbines ranging between 5 to 85 and for case 2 it is between 4 to 85 turbines. Diversity of the solutions can slightly be adjusted and sometimes can be made larger with little alteration of probability of '0' during initialization of decision variables as described in section 3.1. This is merely an information to the readers as diversity achieved in all study cases here are good enough for practical application where occupancy of wind turbines in a windfarm hardly exceeds 50%.

NREL report [18] gives insight of land use requirement of wind power plant in United States based on statistical data. Average area requirement for the power plant is 34.5±22.4 hectare per MW of installed capacity. The range being very wide, we choose two extreme values to make our selection of optimized layouts. Following the guideline, we can have minimum 11 and maximum 50 turbines in the windfarm. From the pool of optimized solutions, we select layouts for 11 turbines for site 1 and site 2, presented in Fig. 9 and Fig. 10 respectively. Fig. 11 and Fig. 12 indicate the optimized layouts of 50 turbines for wind conditions at site 1 and site 2.

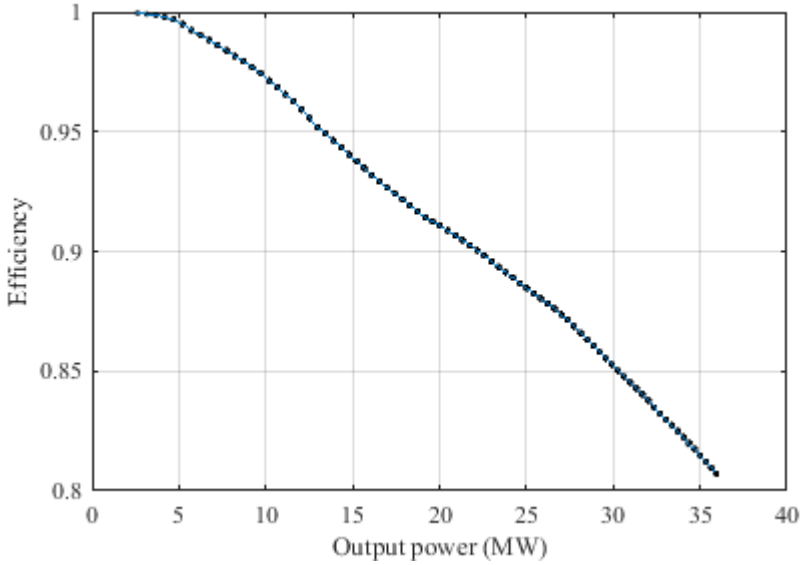

Fig. 5: Plot of *Pareto front* for case 1 (site 1)

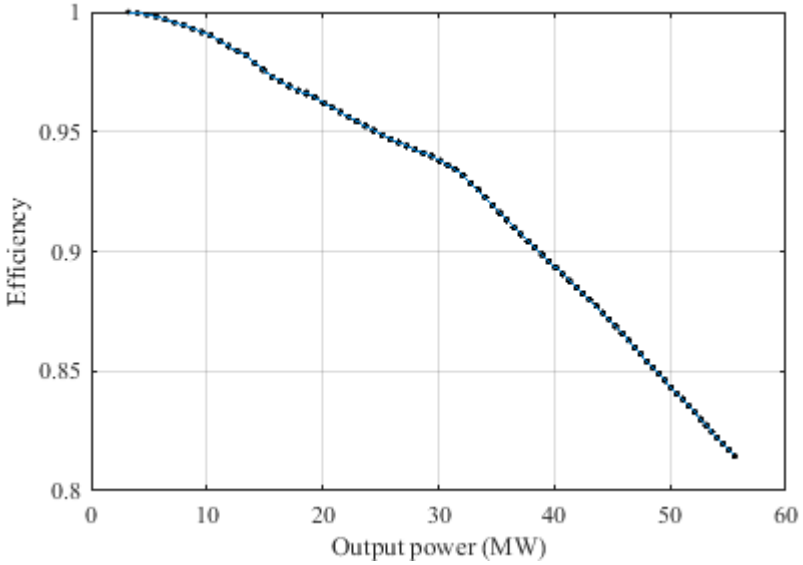

Fig. 6: Plot of *Pareto front* for case 2 (site 2)

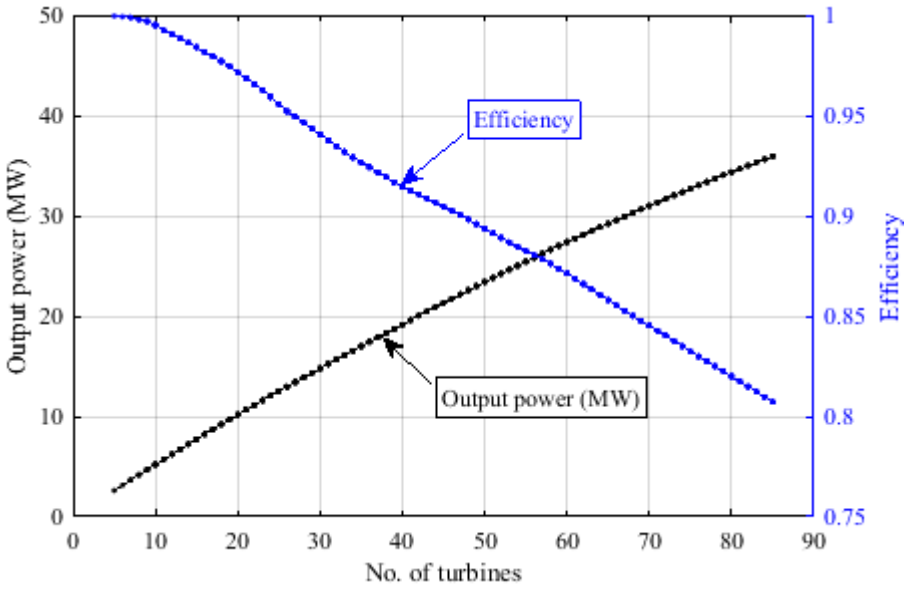

Fig. 7: Variation of output power and efficiency with no. of turbines (case 1, site 1)

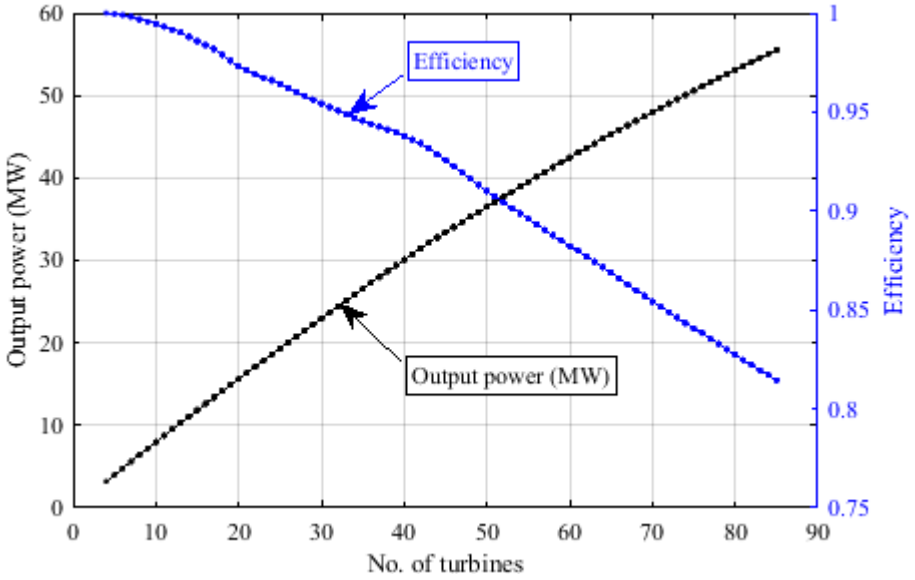

Fig. 8: Variation of output power and efficiency with no. of turbines (case 2, site 2)

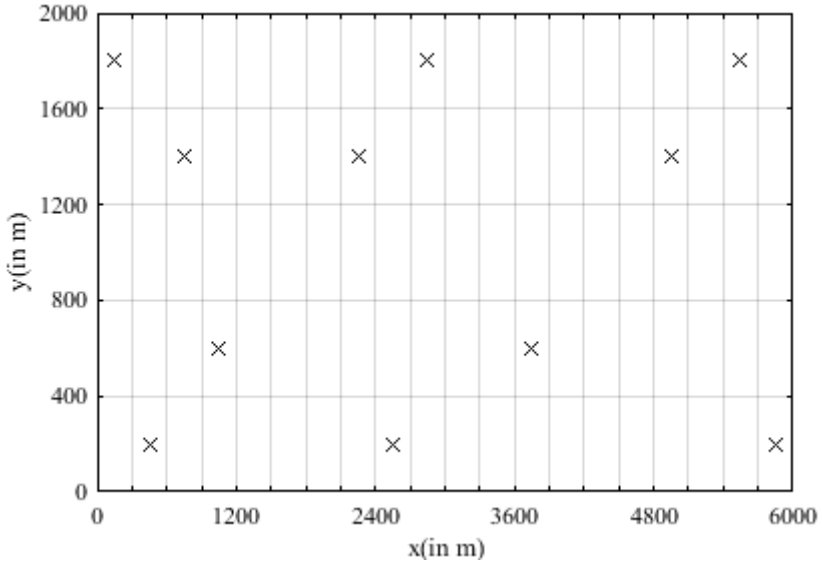

Fig. 9: Optimal layout with 11 turbines (case 1, site 1)

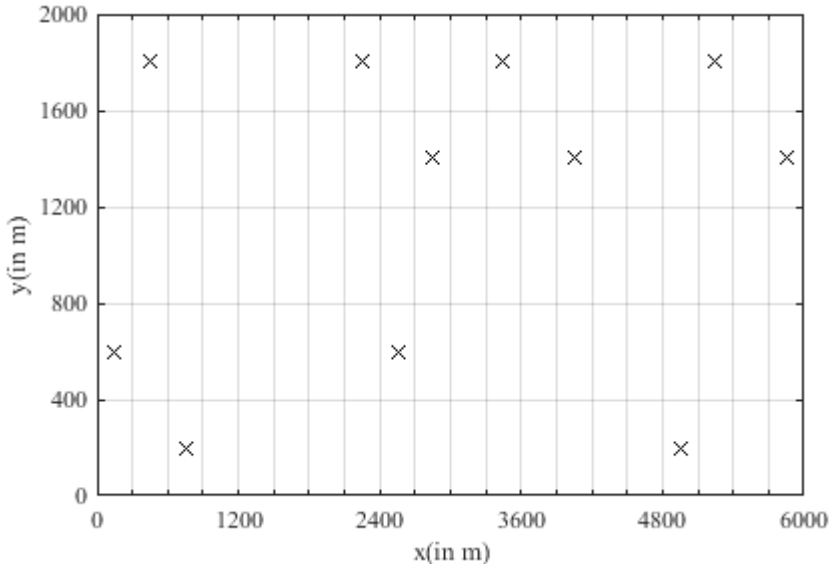

Fig. 10: Optimal layout with 11 turbines (case 2, site 2)

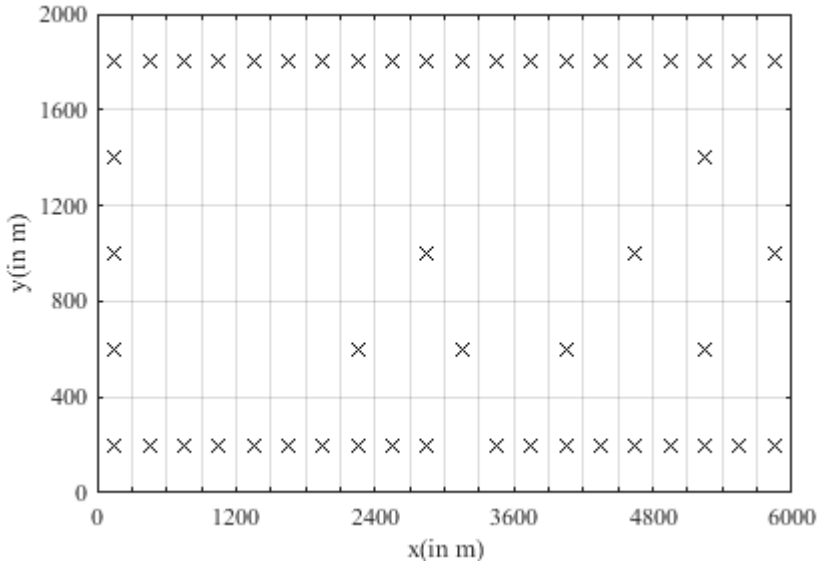

Fig. 11: Optimal layout with 50 turbines (case 1, site 1)

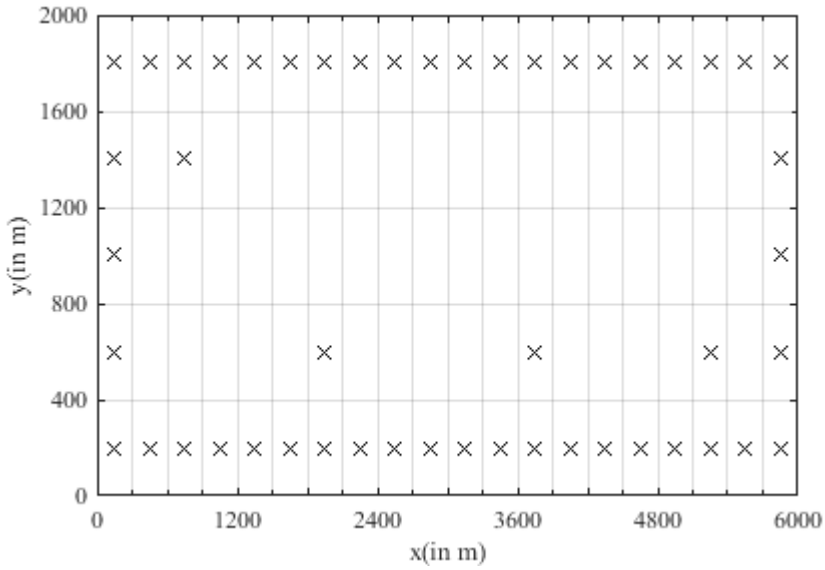

Fig. 12: Optimal layout with 50 turbines (case 2, site 2)

From the optimal layouts, it is evident that turbines try to locate far from each other to minimize wake loss. The algorithm place 11 turbines sparsely at both sites (Fig. 9 and Fig. 10) to achieve very high efficiency of more than 99% as recorded in Table 3. The wind distribution diagram of site 1 reveals that the dominant wind directions are from between south east and south west. Therefore, in Fig. 11, higher concentration of turbines is noticed towards south side. Furthermore, as wind probability is higher from south west direction, all cells at that side are occupied. The turbines at north side allocate themselves at outermost grid to minimize the effect of wake loss when predominant wind direction is from south, thereby forming efficient arrangement.

Wind intensity and probability of occurrence is highest from south east side at site 2. As observed from the optimized layout in Fig. 12, cells at south east sides are all occupied and along that direction turbines are not closely spaced to avoid high wake losses. In both Fig. 11 and Fig. 12, juxtaposition of turbines is observed along east-west direction. Wind probabilities at both the sites are low from east or west direction. Therefore, wake loss for such adjacent placements along east-west direction is far more compensated with sparse allocation of wind turbines along other directions. Further, as wind probabilities from all directions have certain weightage at site 1, the turbines are little more distributed (Fig. 11) than at site 2 (Fig. 12) where turbines are more concentrated. Similar to layouts with 11 and 50 turbines, one can choose any optimized layouts containing an intermediate number of turbines. As mentioned beforehand, the selection is based on required installed capacity, budget, site constraints like land availability, other site auxiliary facilities and feasibility of integration of wind power into the grid. Some results of optimized layouts with different numbers of turbines alongwith corresponding power output and efficiency are listed in Table 3. Power output may seem low compared to the installed capacity. Statistical data reveal that land based modern windfarms operate at annual capacity factor somewhere between 20% to 50% [24,28]. Capacity factor is the amount of energy delivered during a year divided by the amount of energy that would have been generated if the electricity generating source were running at maximum power output throughout the year. Capacity factors thus calculated for the case studies are conclusive and more realistic.

Table 3:
Some optimized layout results for case 1 and case 2

Case 1, site 1				Case 2, site 2			
No. of turbines	Power Output (MW)	Efficiency	Capacity factor	No. of turbines	Power Output (MW)	Efficiency	Capacity factor
10	5.21	99.5%	26.1%	10	7.98	99.5%	39.9%
11	5.72	99.2%	26.0%	11	8.76	99.3%	39.8%
20	10.18	97.1%	25.5%	20	15.61	97.3%	39.0%
30	14.78	94.1%	24.6%	30	22.97	95.4%	38.3%
40	19.16	91.4%	23.9%	40	30.09	93.8%	37.6%
50	23.40	89.4%	23.4%	50	36.50	91.0%	36.5%
60	27.38	87.1%	22.8%	60	42.47	88.2%	35.4%

4.2. Case 3 and case 4 (different hub heights)

In these case studies, different available hub heights (60m, 67m and 78m) of the wind turbines are included in the optimization process. Case 3 utilizes wind data from site 1 while case 4 is performed with site 2 wind data. The algorithm selects required hub heights for the turbines based on optimization objectives of maximizing output power and efficiency. Wind speeds at the reference height are considered same as in case 1 and case 2 i.e. $u_{ref0} <$ 4m/s, $u_{ref1} = 8.2$m/s, $u_{ref2} = 10.8$m/s and $u_{ref3} = 14.4$m/s at $h_{ref} = 60$m. Variation in local wind speed at a different hub height follows logarithmic law in equation (6). Wind velocity in wake, power output and objectives are calculated using equations (1) to (10). The plots of *Pareto fronts* i.e. non-dominated solutions for objectives (total 600 points) of the selected runs are shown in Fig. 13 and Fig. 14 for wind characteristics at site 1 and site 2 respectively. Little more unevenness in the *Pareto fronts* is noted than in study cases with same hub height. One probable explanation is presence of more variants of wind turbines in the optimization process. The objective value changes in an irregular pattern if a single factor out of number of turbines, tower height of the turbine or location changes during function evaluation process. Nevertheless, appropriate trend of dipping efficiency is observed with increase in number of turbines, hence power output. Further, site 2 being more potent to produce wind power, the power output and efficiency are higher for site 2 than for site 1 with same number of turbines.

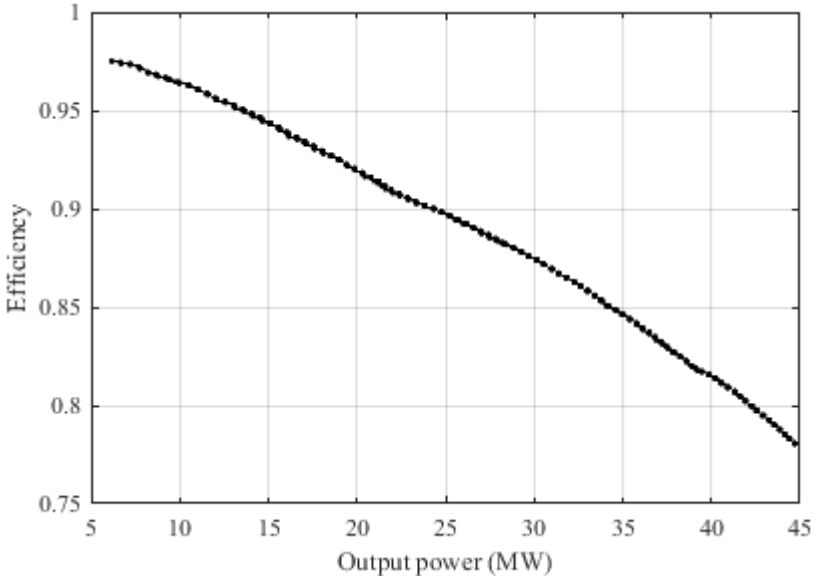

Fig. 13: Plot of *Pareto front* for case 3 (site 1)

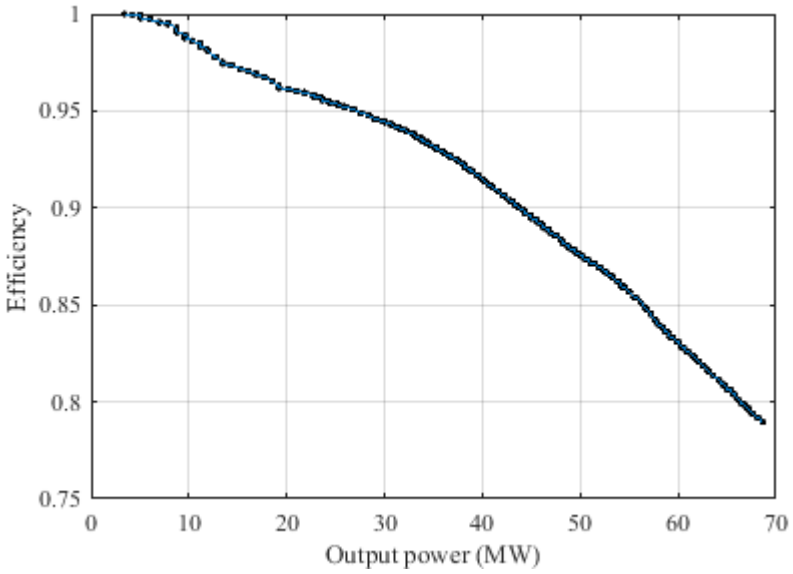

Fig. 14: Plot of *Pareto front* for case 4 (site 2)

Number of turbines for each solution versus the corresponding power output at achievable efficiency is plotted in Fig. 15 for case 3 and Fig. 16 for case 4. Plots in Fig. 17 and Fig. 18 enlighten on distribution of selected hub heights for the *Pareto* solutions in both the cases. For better readability bar charts of selected hub heights at some useful discrete solutions are provided in Fig. 19 and Fig. 20 for case 3 and case 4 respectively. As expected, turbines with highest hub heights are predominantly selected by the algorithm as the same can generate more power at most of the conditions of wind occurrences. When occupancy in the farm gets higher, in some of the optimized layouts the turbines may come close to each other placing themselves in adjacent cells resulting pronounced wake loss. In such cases, a small number of turbines with lower hub heights can be used as power output will not change to a great extent if those are replaced with higher hub heights. Indeed, resulting efficiency might marginally increase with a mix of lower and higher hub heights of turbines in the windfarm as summary in Table 4 reveals. A probable cause linked with the increase in efficiency is the saturation of output power beyond a certain wind speed. To elaborate, increase in hub height means available wind speed at hub height and thus wind power is higher. But actual power output from the turbine does not increase to the same extent due to either wake loss or saturation of turbine output. The statement is further clarified during analysis of optimal layouts obtained with different numbers of turbines for the two wind conditions.

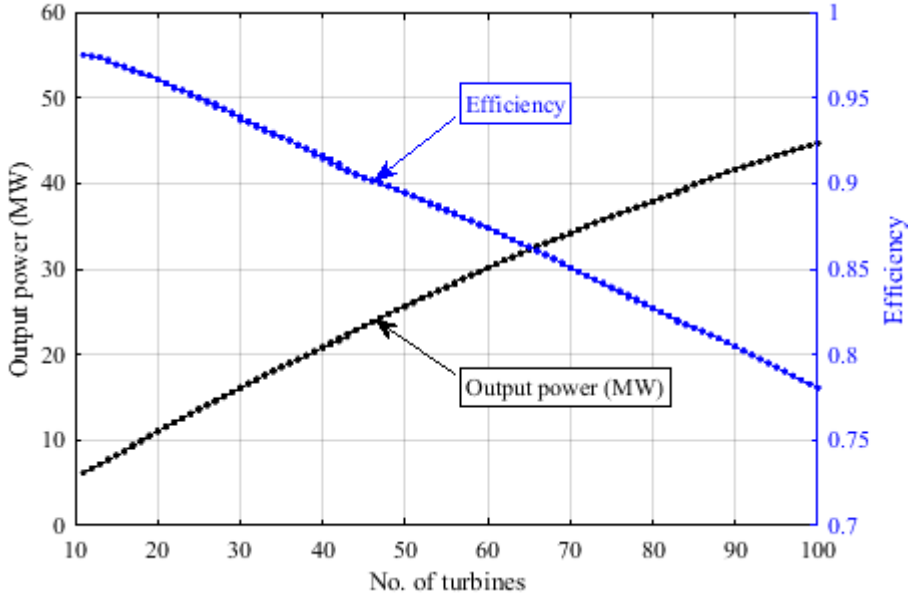

Fig. 15: Variation of output power and efficiency with no. of turbines (case 3, site 1)

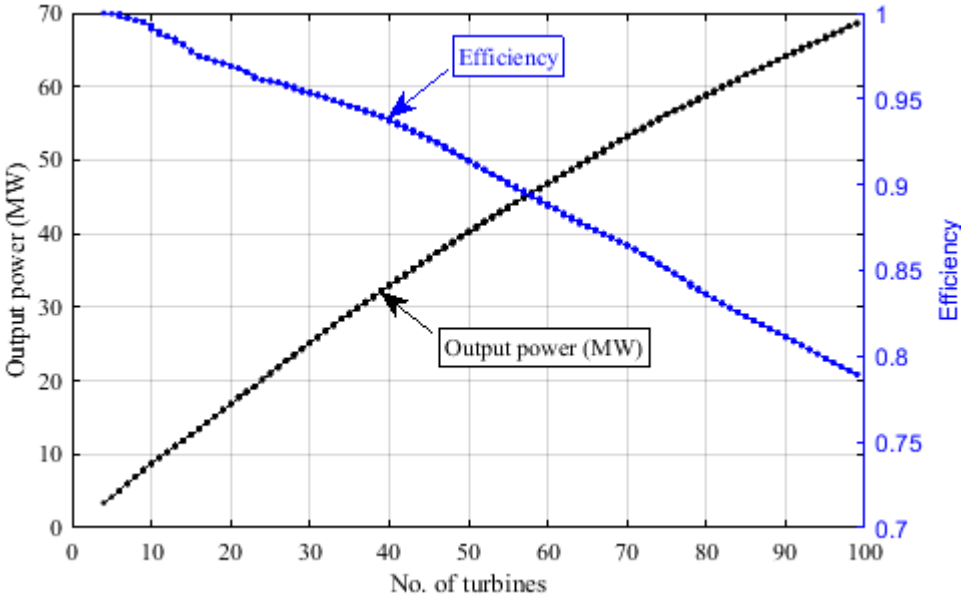

Fig. 16: Variation of output power and efficiency with no. of turbines (case 4, site 2)

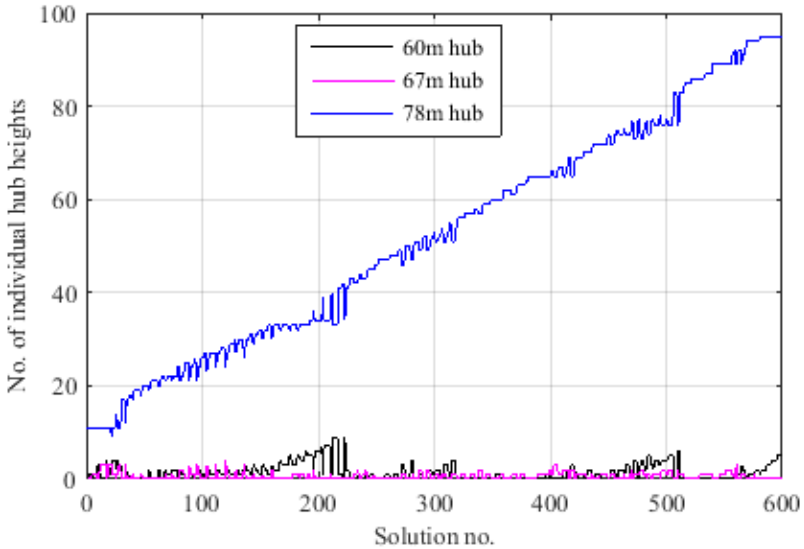

Fig. 17: Plot of selected hub heights for optimal solutions (case 3, site 1)

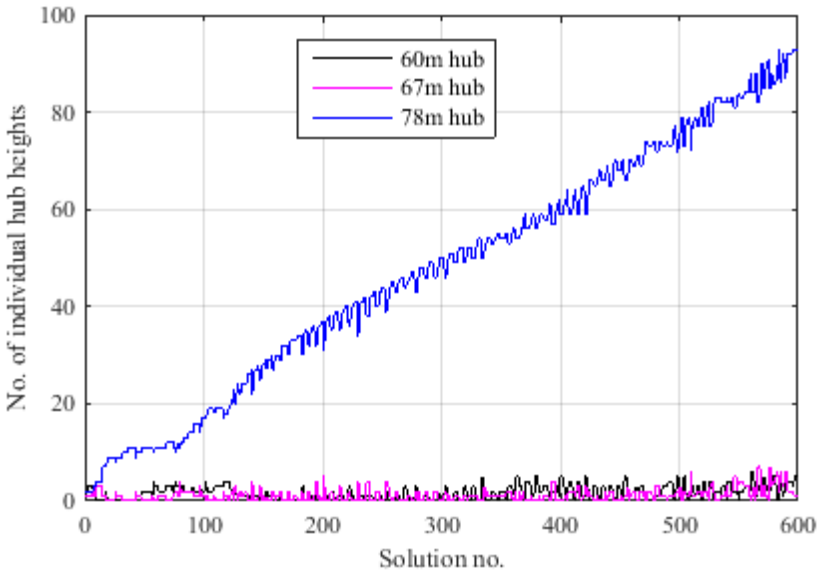

Fig. 18: Plot of selected hub heights for optimal solutions (case 4, site 2)

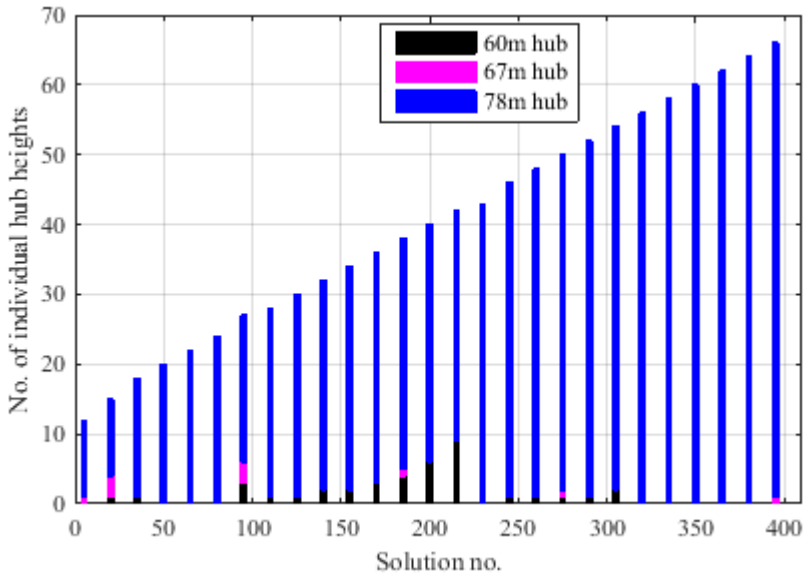

Fig. 19: Selected hub heights at some discrete optimal solutions (case 3, site 1)

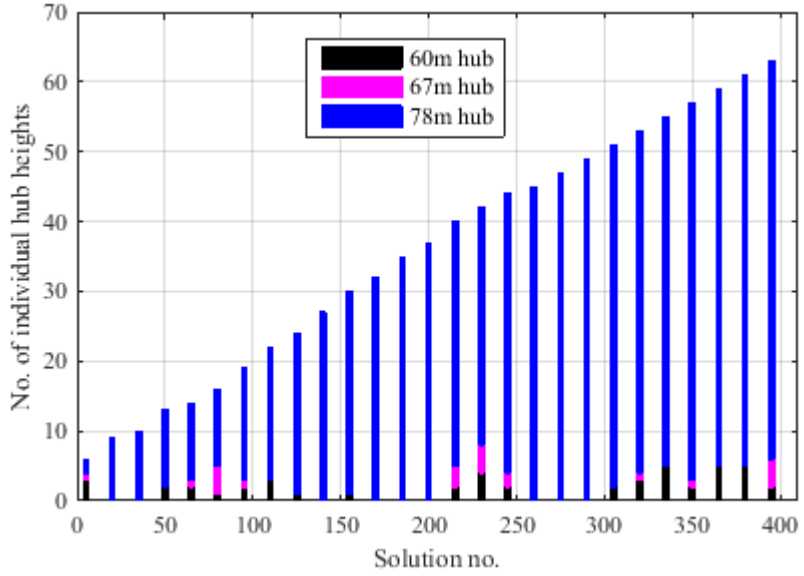

Fig. 20: Selected hub heights at some discrete optimal solutions (case 4, site 2)

Following same reasoning mentioned in case 1 and case 2, our selection of optimized layouts consists of 11 and 50 turbines for case 3 and case 4. Fig. 21 and Fig. 22 represent the optimized layouts with 11 turbines for wind conditions at site 1 and site 2 respectively. Expectedly the algorithm selects all tallest towers for the turbines and layouts are dispersed to minimize wake loss. As listed in Table 4, the higher efficiency in case 4 than in case 3 is due to higher intensity and probability of wind at site 2 than at site 1. Optimized layouts for the two cases with 50 turbines are provided in Fig. 23 and Fig. 24. Similar to case 1, turbines are a bit more distributed in case 3 for site 1. Due to much higher probabilities of wind from certain directions at site 2, the turbines are more concentrated in case 4. It is worthwhile to note that only one variant of layout with 50 turbines is presented here. Table 4 records some more results of arrangements with 50 turbines. All 78m high turbines can generate maximum power output with insignificant reduction in efficiency for reason stated earlier. The user has the flexibility to do some trade-off between the two objectives and select a solution suit to his requirement. Not only that, as optimal layouts are available for each discrete number of turbines over a wide range (e.g. from 4 to 99 in case 4), during design stage one can easily manipulate the plot plan in case a turbine is required to be added or removed.

The metaheuristics applied on windfarm layout optimization till date could find only one optimal layout either with single objective or with a fixed number of turbines. The superiority of MOEA/D and its application in windfarm layout proposed in this paper can provide hundreds of usable solutions in single run of the algorithm. Though it cannot forthrightly be claimed that no solution proposed by MOEA/D can be improved. Indeed, no metaheuristic can make such an authoritative statement. However, the solutions proposed by MOEA/D are among the best and notable improvement of these solutions is difficult by mere trial and error method.

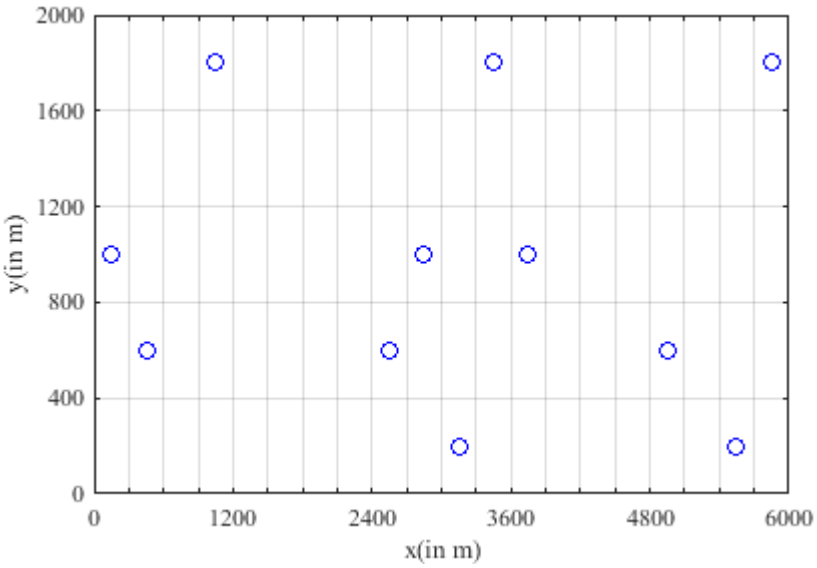

Fig. 21: Optimal layout with 11 turbines (case 3, site 1)

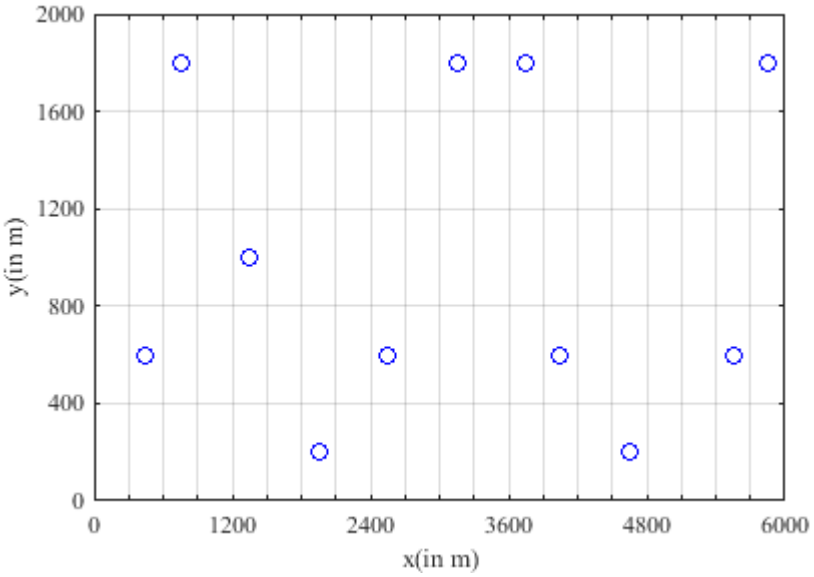

Fig. 22: Optimal layout with 11 turbines (case 4, site 2)

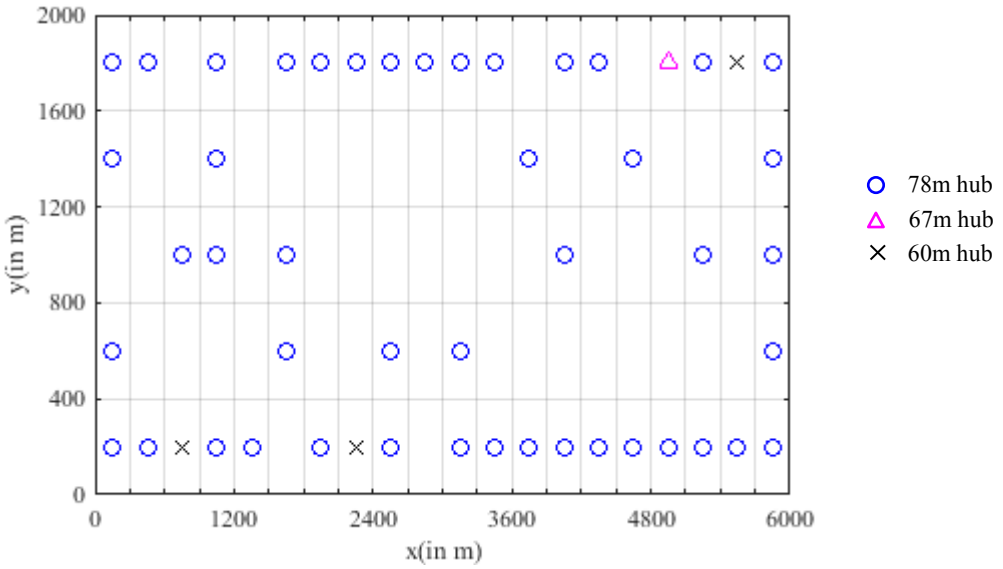

Fig. 23: Optimal layout with 50 turbines (case 3, site 1)

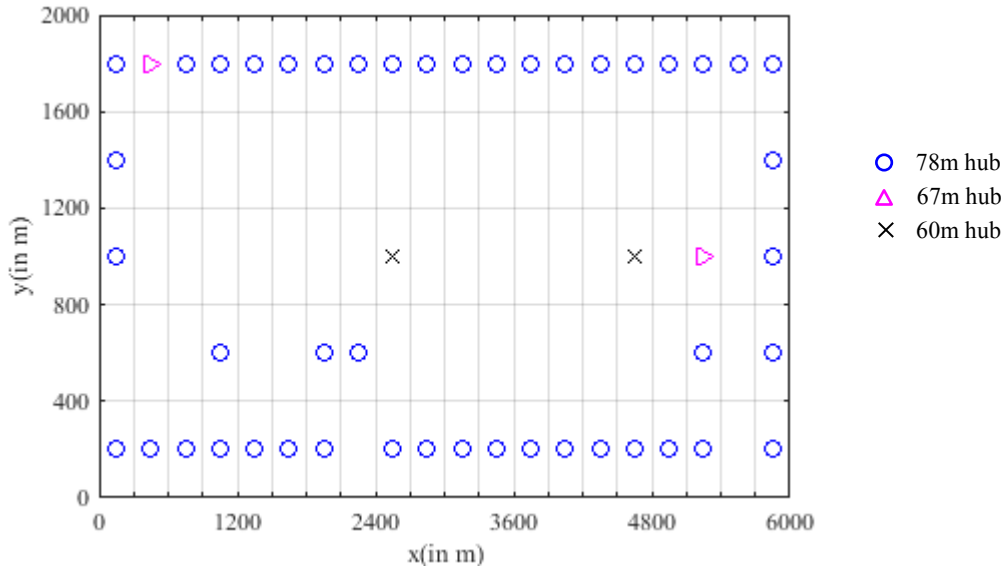

Fig. 24: Optimal layout with 50 turbines (case 4, site 2)

Table 4:
Some optimized layout results for case 3 and case 4

Case 3, site 1							Case 4, site 2						
No. of turbines	Power (MW)	Efficiency	Capacity factor	Selected hub heights			No. of turbines	Power (MW)	Efficiency	Capacity factor	Selected hub heights		
				60m	67m	78m					60m	67m	78m
11	6.17	97.50%	28.0%	0	0	11	11	9.60	98.93%	43.6%	0	0	11
20	10.97	96.07%	27.4%	1	1	18	20	16.74	96.93%	41.8%	3	3	14
20	11.05	96.05%	27.6%	0	0	20	20	16.90	96.89%	42.2%	2	1	17
30	16.00	93.90%	26.7%	2	4	24	30	25.17	95.38%	41.9%	1	0	29
30	16.16	93.66%	26.9%	0	0	30	30	25.22	95.28%	42.0%	0	0	30
40	20.80	91.61%	26.0%	6	0	34	40	32.92	93.81%	41.1%	2	1	37
40	20.98	91.40%	26.2%	1	0	39	40	33.07	93.70%	41.3%	0	0	40
45	23.31	90.36%	25.9%	1	1	43	45	36.56	92.70%	40.6%	1	4	40
45	23.36	90.28%	26.0%	0	0	45	45	36.78	92.62%	40.9%	0	0	45
50	25.56	89.45%	25.6%	3	1	46	50	40.10	91.42%	40.1%	2	2	46
50	25.65	89.44%	25.6%	1	1	48	50	40.14	91.41%	40.1%	2	1	47
50	25.72	89.43%	25.7%	0	0	50	50	40.31	91.37%	40.3%	0	0	50
60	30.13	87.40%	25.1%	0	1	59	60	46.87	88.75%	39.1%	1	1	58
60	30.16	87.40%	25.1%	0	0	60	60	46.91	88.75%	39.1%	1	0	59

Table 4 lists some of the optimized layouts with specific number of turbines. In general, it is observed that using variable hub height is not hugely beneficial. Change in output power and efficiency is marginal. So, for practical convenience in design, logistics, future operation and maintenance, windfarm with turbines of same hub height is a preferred choice with the presumption that reduction of a few hub heights does not significantly affect the levelized cost of energy (LCOE).

5. Conclusion

This paper proposes an effective application and efficient approach to discrete location optimization problem employing multi-objective evolutionary algorithm, different from simplified single objective or weighted sum multi-objective optimization methods suggested by other researchers. The process of optimization outputs most efficient layouts with any selected number of turbines within a specified range. The method can also be applied for selection of different hub heights in search of optimized layout. A single run of the optimization algorithm outputs several closely matched solutions providing more flexibility and choices for windfarm layouts. Review of case studies, specifically of case 3 and case 4, reveals that the algorithm proposes several options for the layouts with same number of turbines. It may be noted that only few alternatives with same number of turbines are listed in Table 4. The algorithm indeed proposes more options for the layouts. Optimal placement of wind turbines is a complex task as several factors affect the overall performance and output from the windfarm. The objectives of the algorithm can be twisted or altered based on the importance exercised on several governing factors. Moreover, if actual cost data are available, new objective of cost can also be integrated into the optimization algorithm. A bi-objective formulation with cost and output power would help to easily determine the rate of change in cost with the installed capacity or output power. A tri-objective formulation with output power, windfarm efficiency and cost is also probable. In a multi-objective optimization problem, the designer should always perform trade-off among the objectives involved in the optimization. No matter what or how many the objectives are, the approach of wind turbine location optimization can be followed the way proposed in this paper.

Acknowledgement: This project is funded by the National Research Foundation Singapore under its Campus for Research Excellence and Technological Enterprise (CREATE) program.

References

[1]. Mosetti, G., Carlo Poloni, and B. Diviacco. "Optimization of wind turbine positioning in large windfarms by means of a genetic algorithm." *Journal of Wind Engineering and Industrial Aerodynamics* 51.1 (1994): 105-116.

[2]. Grady, S. A., M. Y. Hussaini, and Makola M. Abdullah. "Placement of wind turbines using genetic algorithms." *Renewable energy* 30.2 (2005): 259-270.

[3]. Mittal, Anshul. *Optimization of the layout of large wind farms using a genetic algorithm*. Diss. Case Western Reserve University, 2010.

[4]. Emami, Alireza, and Pirooz Noghreh. "New approach on optimization in placement of wind turbines within wind farm by genetic algorithms." *Renewable Energy* 35.7 (2010): 1559-1564.

[5]. Marmidis, Grigorios, Stavros Lazarou, and Eleftheria Pyrgioti. "Optimal placement of wind turbines in a wind park using Monte Carlo simulation." *Renewable energy* 33.7 (2008): 1455-1460.

[6]. Pookpunt, Sittichoke, and Weerakorn Ongsakul. "Optimal placement of wind turbines within wind farm using binary particle swarm optimization with time-varying acceleration coefficients." *Renewable Energy* 55 (2013): 266-276.

[7]. Biswas, Partha P., P. N. Suganthan, and Gehan AJ Amaratunga. "Optimal placement of wind turbines in a windfarm using L-SHADE algorithm." *Evolutionary Computation (CEC), 2017 IEEE Congress on*. IEEE, 2017.

[8]. Eroğlu, Yunus, and Serap Ulusam Seçkiner. "Design of wind farm layout using ant colony algorithm." *Renewable Energy* 44 (2012): 53-62.

[9]. Chen, K., M. X. Song, Z. Y. He, and X. Zhang. "Wind turbine positioning optimization of wind farm using greedy algorithm." *Journal of Renewable and Sustainable Energy* 5, no. 2 (2013): 023128.

[10]. Chen, K., Song, M. X., Zhang, X., & Wang, S. F. (2016). Wind turbine layout optimization with multiple hub height wind turbines using greedy algorithm. *Renewable Energy*, *96*, 676-686.

[11]. González, Javier Serrano, Angel G. Gonzalez Rodriguez, José Castro Mora, Jesús Riquelme Santos, and Manuel Burgos Payan. "Optimization of wind farm turbines layout using an evolutive algorithm." *Renewable energy* 35, no. 8 (2010): 1671-1681.

[12]. DuPont, Bryony, Jonathan Cagan, and Patrick Moriarty. "An advanced modeling system for optimization of wind farm layout and wind turbine sizing using a multi-level extended pattern search algorithm." *Energy* 106 (2016): 802-814.

[13]. Biswas, Partha P., P. N. Suganthan, and Gehan AJ Amaratunga. "Optimization of Wind Turbine Rotor Diameters and Hub Heights in a Windfarm Using Differential Evolution Algorithm." *Proceedings of Sixth International Conference on Soft Computing for Problem Solving*. Springer, Singapore, 2017.

[14]. Chen, Ying, Hua Li, Bang He, Pengcheng Wang, and Kai Jin. "Multi-objective genetic algorithm based innovative wind farm layout optimization method." *Energy Conversion and Management* 105 (2015): 1318-1327.

[15]. Feng, Ju, Wen Zhong Shen, and Chang Xu. "Multi-objective random search algorithm for simultaneously optimizing wind farm layout and number of turbines." *Journal of Physics: Conference Series*. Vol. 753. No. 3. IOP Publishing, 2016.

[16]. Zhang, Qingfu, and Hui Li. "MOEA/D: A multiobjective evolutionary algorithm based on decomposition." *IEEE Transactions on evolutionary computation* 11.6 (2007): 712-731.

[17]. Zhang, Qingfu, Wudong Liu, and Hui Li. "The performance of a new version of MOEA/D on CEC09 unconstrained MOP test instances." *IEEE congress on evolutionary computation*. Vol. 1. 2009.
[18]. Denholm, Paul, et al. "Land-use requirements of modern wind power plants in the United States." *Golden, Colorado: National Renewable Energy Laboratory* (2009).
[19]. https://www.tceq.texas.gov/airquality/monops/windroses.html
[20]. Jensen, Niels Otto. *A note on wind generator interaction*. 1983.
[21]. Katic, I., J. Højstrup, and Niels Otto Jensen. "A simple model for cluster efficiency." *European Wind Energy Association Conference and Exhibition*. 1986.
[22]. International Electrotechnical Commission. "IEC 61400-1: Wind turbines part 1: Design requirements." *International Electrotechnical Commission* (2005).
[23]. Chen, Y., Li, H., Jin, K., & Song, Q. (2013). Wind farm layout optimization using genetic algorithm with different hub height wind turbines. *Energy Conversion and Management*, *70*, 56-65.
[24]. Moné, C., et al. *Cost of Wind Energy Review*. NREL/TP-5000-63267. Golden, Colorado: National Renewable Energy Laboratory, 2013.
[25]. Tong, Weiyang, et al. "Impact of different wake models on the estimation of wind farm power generation." *12th AIAA Aviation Technology, Integration, and Operations (ATIO) Conference and 14th AIAA/ISSMO Multidisciplinary Analysis and Optimization Conference, American Institute of Aeronautics and Astronautics*. 2012.
[26]. Miettinen, Kaisa. *Nonlinear multiobjective optimization*. Vol. 12. Springer Science & Business Media, 2012.
[27]. Zhao, Shi-Zheng, Ponnuthurai Nagaratnam Suganthan, and Qingfu Zhang. "Decomposition-based multiobjective evolutionary algorithm with an ensemble of neighborhood sizes." *IEEE Transactions on Evolutionary Computation* 16.3 (2012): 442-446.
[28]. European Wind Energy Association. *The economics of wind energy*. EWEA, 2009.
[29]. Biswas, P. P., Mallipeddi, R., Suganthan, P. N., & Amaratunga, G. A. (2017). A multiobjective approach for optimal placement and sizing of distributed generators and capacitors in distribution network. *Applied Soft Computing*.